Malaysian Journal of Analytical Sciences (MJAS)
Published by Malaysian Analytical Sciences Society

ANALYSIS OF EFFLORESCENCE OF SPENT BLEACHING CLAY BASED GEOPOLYMER USING ALKALINE LEACHABILITY METHODS

(Analisa Peroian Geopolimer Berasaskan Tanah Liat Terluntur Menggunakan Kaedah Kelarutlesapan Alkali)

Puuvina Jeyasangar, Mohd Hazwan Hussin, and Shangeetha Ganesan*

School of Chemical Sciences, Universiti Sains Malaysia, 11800 USM, Pulau Pinang, Malaysia

**Corresponding author: shangeetha@usm.my*

Received: 1 September 2023; Accepted: 15 February 2024; Published: 29 April 2024

Abstract

Geopolymers are a class of inorganic amorphous polymeric materials made up of silica, alumina and alkali- metal oxides. The presence of alkali in the geopolymer formulation aids in the dissolving of aluminosilicate precursors, resulting in the creation of microstructures and increases geopolymer strength. However, the alkali content is the most critical factor influencing efflorescence production. Therefore, this study evaluated the effects of curing parameters on efflorescence formation on spent bleaching clay based geopolymer. The efflorescence effects were analysed by alkaline leachability methods using atomic absorption spectroscopy (AAS) and electrochemical impedance spectroscopy (EIS). Neat geopolymer as well as cured geopolymer with different liquid/solid (L/S) ratio effects were studied. Alkaline leaching studies revealed water-cured geopolymers with liquid/solid (L/S) ratio of 2:1 shows that 974.9 ppm Na^+ ions leached from the geopolymer. This method helps to prevent efflorescence from reoccurring as most of the free Na^+ ions has already been leached from the geopolymer sample. The EIS analysis also showed that a 2:1 ratio had excellent resistance which reflects the mobility of the other ions such as silicon, aluminium and chloride ions. Functional group analysis using FTIR demonstrated the key peaks involved in development of geopolymer from spent bleaching clay (SBC) such as v(Si-O-Si / Si-O-Al) (bending & stretching), v(Al-O)(symmetrical), v(Si-O / Al-O) (asymmetrical) and v(O-H). Surface morphology analysis using SEM-EDX indicates that adequate silica-rich components were required to increase the mechanical strength of geopolymers by densifying their microstructure with more bulk and compact layers. From the examination of thermal stability of neat and treated geopolymer compositions decomposed at 700 °C confirming the thermal resistance of the material. Therefore, for more sustainable cements, alkali leachability can be performed on SBC-based geopolymer by water-curing as it revealed to have an exceptional performance on total Na leached, resistance and thermal stability as shown in this study.

Keywords: geopolymer, spent bleaching clay, efflorescence, leachability

Abstrak

Geopolimer adalah kelas bahan polimer amorfus tidak organik yang terdiri daripada silika, alumina dan logam-alkali oksida. Kehadiran alkali dalam formula geopolymer membantu dalam pelarutan bahan pemula aluminosilika, menghasilkan mikrostruktur serta menguatkan struktur geopolimer. Akan tetapi, kandungan alkali adalah faktor yang paling kritikal yang mempengaruhi pembentukan peroi. Oleh itu, kajian ini adalah untuk menilai sintesis geopolimer daripada tanah liat terluntur dan menganalisa peroian dengan kaedah kelarutanlesapan menggunakan AAS dan EIS. Geopolimer tulen serta geopolimer yang

dirawat dengan kesan nisbah cecair/pepejal (L/S) yang berbeza telah dikaji. Kajian kelarutlesapan alkali menunjukkan geopolimer yang diawet dengan air pada nisbah air/pepejal (L/S) 2:1 menghasilkan 974.9 ppm Na^+ ions melarutlesap daripada geopolimer tersebut. Cara ini mencegah pembentukkan peroi daripada berulang kerana kebanyakkan ion Na^+ bebas telah dilarutlesap daripada geopolimer. Analisa EIS menunjukkan bahawa nisbah 2:1 juga mempunyai rintangan yang baik yang mencerminkan pergerakan ion-ion yang lain seperti silicon, aluminium dan klorida. Analisa kumpulan fungsi menggunakan FTIR menunjukkan puncak-puncak utama yang terlibat dalam penghasilan geopolimer berasaskan tanah liat (SBC) yang terdiri daripada v(Si-O-Si / Si-O-Al) (bengkok & regangan), v(Al-O) (simetri), v(Si-O / Al-O) (tidak simetri) dan v(O-H). Analisis morfologi permukaan mengunakan SEM-EDX menunjukkan bahawa komponen kaya silika yang mencukupi diperlukan untuk meningkatkan kekuatan mekanikal geopolimer dengan memadatkan struktur mikronya dengan lebih banyak lapisan pukal dan padat. Daripada pemeriksaan kestabilan terma komposisi geopolimer yang asal dan dirawat itu terurai pada suhu 700°C menunjukkan kerintangan haba mereka. Oleh itu, untuk simen yang lebih mampan, kelarutlesapan alkali boleh dilakukan pada geopolimer berasaskan SBC dengan pengawetan air kerana ia menunjukkan prestasi yang luar biasa berdasarkan jumlah Na yang kelarutlesapan serta kestabilan termanya seperti yang dibuktikan dalam penyelidikan ini.

Kata kunci: geopolimer, tanah liat terluntur, peroian, kelarutlesapan

Introduction

Geopolymers or inorganic polymers, have excellent potential for industrial applications as they are both environmentally friendly and possess unique physico-chemical characteristics [1]. Geopolymers are alternative binder for fibre composites and cement for concrete that have outstanding physical, chemical, and mechanical prospects. They can also be employed in a variety of applications due to their outstanding physical properties, which include fire, heat, acid, and corrosion resistance, as well as high compressive strength. Fire-resistant and thermal-insulating materials, also low-tech and low- energy materials like cements, concretes and tiles are amongst them [2]. The appearance of efflorescence on geopolymer surfaces, independent of the precursor utilised, is a significant impediment to the application of geopolymer products. The formation of efflorescence might cause the geopolymer structure to deteriorate. The formation of efflorescence is linked to the leaching of sodium ion from geopolymers when the product encounters moisture or water. The material leaches alkali ions and transport them to the surface via capillary forces. These ions combine with carbon dioxide (CO_2) in the environment to generate hydrated sodium carbonate (Na_2CO_3) when the water evaporates. This takes effect notably when the material contains an excessive amount of alkaline substances which also has a high porosity [3]. Sodium hydroxide (NaOH) is extensively utilised during geopolymer synthesis as compared to potassium hydroxide (KOH) as NaOH optimises the dissolution procedure along with the combination of silicate solution [4]. This process is important since the solubility of aluminosilicate increases as the concentration of hydroxide increases. Geopolymer concrete with a greater NaOH concentration has a better compressive strength [5].

Numerous aluminosilicate substances are present in nature and some of them are also produced from industry wastes [6]. Spent bleaching clay (SBC) is a solid waste product from the refinement of palm oil where the disposal of bleaching clay as a byproduct from refining plants causes several environmental issues as well as financial losses to the country [7]. Spent bleaching clay (SBC) contains between 20-40% residual oil that may be a fire hazard [8]. Spent bleaching clay (SBC) is mostly made of SiO_2 followed by Al_2O_3, MgO, Fe_2O_3 and CaO, whilst its elemental components are C, Ca, O, Fe, Mg, Al, Si, P and K [9,10]. Besides, the main component utilised in this research is montmorillonite, which is a bentonite clay, with the potential to absorb several times its size, taking on a jelly-like consistency due to the hydration upon contact with aqueous solutions. Therefore, giving it a capacity for ion sorption, which can be improved by conducting an alkaline activation that results in the formation of a geopolymer or inorganic polymer.

As afore mentioned, the alkali concentration is vital to produce geopolymeric gels and to enhance the strength of the synthesised geopolymer [11]. Nevertheless, the alkali metals are weakly attached in the matrix and can readily be leached away in water. Thus, resulting in development of white efflorescence (Na_2CO_3) on the surface of the geopolymer, when it is in contact with water and moisture. This subsequently has a major

effect on degradation of geopolymer cements [12]. Furthermore, efflorescence on geopolymer surfaces, whether made of montmorillonite, metakaolin, fly ash, volcanic tuff, or other aluminosilicate precursors, is a significant hurdle for their utilisation [3]. Therefore, this work strategises towards the target of studying efflorescence formation by evaluating the amount of Na^+ leached using AAS and EIS are vital for future construction science.

It is hypothesised that the SBC-based geopolymer demonstrates greater physicochemical properties. However, excess efflorescence may disrupt the stability of the binder microstructure, which has been a persistent drawback in the development of geopolymers as reported in previous studies [3,12]. The characterisation techniques are used to support the formation of geopolymer from spent bleaching clay. This work develops the variation in curing conditions as the principal motive to study the development of efflorescence for the novel spent bleaching clay based geopolymer which has not been reported elsewhere.

Materials and Methods

Reagents and raw materials

Chemicals, reagents, and solvents employed in this investigation, specifically sodium hydroxide (NaOH), sodium silicate (Na_2SiO_3), sodium chloride (NaCl) were commercially purchased from local suppliers as analytical reagents such as Systerm, QReC and R&M Chemicals. They were utilised exactly as they are, with no further purification. Furthermore, all reactions were carried out in an ambient environment. While, spent bleaching clay was contributed by KL Kepong Oleomas Sdn Bhd, Selangor.

Geopolymer synthesis

Geopolymer was synthesised with starting materials, 15.6633g of NaOH and 54.8213g of Na_2SiO_3 mixed in 150 mL distilled water respectively. The ratio of the starting materials were NaOH : Na_2SiO_3 = 1 : 3.5, also known as the alkaline activator solution. The geopolymer paste and composites were attained by mixing the alkaline activator solution into 160.0g of SBC gradually. Empirically, the geopolymer composite complied to the ratio of alkaline activating solution (NaOH + Na_2SiO_3) : SBC of 1 : 2.27 [11,13]. Then, the composite was poured into molds and left in the oven at 70°C for 24 hours; conducive for curing process in to accelerate the gel formation [13,14]. Then, the geopolymer paste was left to undergo a hardening process for a week before proceeding with subsequent steps.

Characterisation of geopolymer

Perkin Elmer 100 FT-IR spectroscopy was utilised for FT-IR analysis by employing potassium bromide (KBr) pellets within spectral range 4000-400 cm^{-1} for determination of functional group in the synthesised geopolymer. In addition, for image analysis, Zeiss GeminiSEM 360 Field Emission Scanning Electron Microscope (FESEM) was utilised to examine the morphological phases. The characterisation techniques are important to showcase the formation of the geopolymer before the leaching study can be conducted.

Alkaline leaching test

Leaching test was conducted on the geopolymers to determine the alkaline leachability after 28 days of immersion test via AAS and EIS [15]. The leaching process was examined in two different conditions which were ambient curing and water curing, as per Table 1. Demolded geopolymers were placed in larger containers and sealed for ambient curing meanwhile, for water curing, the study progressed by immersing demolded geopolymer into distilled water in sealed containers for 28 days. The liquid/solid (L/S) for water curing varied from 2:1, 4:1, 10:1 and 20:1 to fully get rid of sodium ions from geopolymer sample. Ambient cured sample was immersed in water to collect the leachate for testing. The ratio of L/S was calculated based on previous study [11]. Thermogravimetric-differential thermal analysis (TGA-DTA) was explored to examine the mass loss as temperature rises. The test proceeded with a heating rate of 10°C/min from ambient temperature to 900°C. All untreated and treated geopolymer samples were evaluated for thermal stability.

Alkaline leachability study via AAS

After 28 days, the samples were analysed by Atomic Absorption Spectroscopy (AAS) for total amount of sodium ions (Na^+) leached. Initially, AAS instrument

was calibrated by using standard solution of 1, 2, 3, 4 and 5 ppm of NaCl, prepared from stock solution of 100 ppm. The standards were run, and a calibration graph was plotted. It is ensured that the $R^2 \geq 0.99$ prior to sample readings. Then, all the leachate of the water cured samples were examined and evaluated.

Table 1. Alkaline leaching sample details according to its curing condition

Curing Conditions	Liquid-to-Solid Ratio (L/S)	Sample
Water curing	2:1	A
	4:1	B
	10:1	C
	20:1	D
Ambient curing	N/A	E

Alkaline leachability study via AAS

After 28 days, the samples were analysed by Atomic Absorption Spectroscopy (AAS) for total amount of sodium ions (Na^+) leached. Initially, AAS instrument was calibrated by using standard solution of 1, 2, 3, 4 and 5 ppm of NaCl, prepared from stock solution of 100 ppm. The standards were run, and a calibration graph was plotted. It is ensured that the $R^2 \geq 0.99$ prior to sample readings. Then, all the leachate of the water cured samples were examined and evaluated.

Alkaline leachability study via EIS

Impedance of the geopolymer samples from different curing conditions as per Table 1 were measured by the electrochemical impedance spectroscopy (EIS), Gamry Reference 600 electrochemical workstation with three electrode setups. First, the electrodes utilised were platinum as counter electrode (CE), graphite as working electrode (WE) and saturated calomel electrode (SCE) as reference electrode (RE). These electrodes were immersed in a beaker which contained a leached liquid sample of geopolymers from different curing conditions. Then, the Gamry Reference600 electrochemical workstation was opened to test the EIS with the frequency range set at 10^{-1} to 10^5 while AC amplitude of 10mV. The resulted Nyquist plots were analysed further.

Results and Discussion

Synthesis of geopolymer

Geopolymer was synthesized and characterized as an alternate new cement for concrete instead of ordinary Portland Cement (OPC). The preparation of geopolymer was accomplished via geopolymerisation process through aluminosilicate material dissolved in 0.39 mol of sodium hydroxide and 0.45 mol of sodium silicate to attain geopolymer and a by-product which is water molecules as shown in Figure 1.

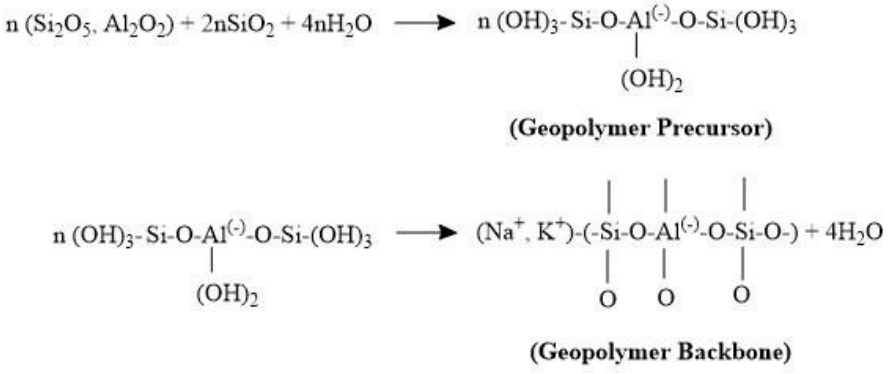

Figure 1. Mechanism of geopolymer synthesis [15]

Principally, the geopolymerisation technique consists of three main mechanisms [16]. Firstly, the dissolution of aluminosilicate materials in alkaline media by the breaking of covalent Si-O-Si and Al-O-Al bonds, resulting in the production of silicate and aluminate species. The hydroxyl (OH-) groups commence this process by attaching to the silicon atom, making the Si-O-Si bond more prone to breaking. At high pH, reactive aluminosilicates will dissolve quickly. Then, condensation of silicate and aluminate monomers will develop a gel until the solution approaches saturation, resulting in the release of NaOH, which reacts again. Finally, the gel undergoes polycondensation and structural rearrangement, resulting in a 3-D aluminosilicate structure of geopolymers. The final compound attained in this study is medium deep brown as shown in Figure 2. Physically, the cementitious geopolymer showed slight amount of efflorescence on its surface after aging for 28 days. There is no visible pore spotted on the surface of synthesised geopolymer.

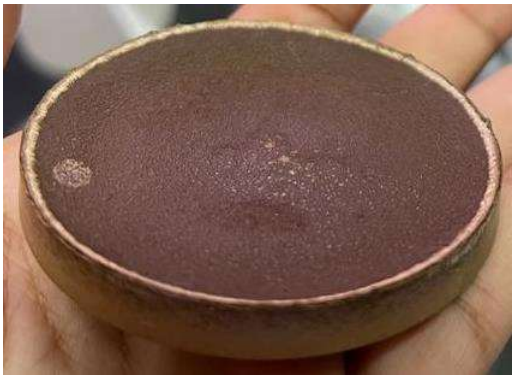

Figure 2. Geopolymer synthesized and aged for 28 days at room temperature

Functional group analysis

Functional group analysis of SBC and SBC-based geopolymer revealed all the expected bands of interest namely v(Si-O-Si / Si-O-Al) (bending), v(Si-O-Si / Si-O-Al) (stretching), v(Al-O) (symmetrical), v(Si-O / Al-O) (asymmetrical) and v(O-H) as seen in Figure 3. The spectrum ranging from strong intensity of SBC to moderate intensity of SBC-based geopolymer synthesised in this study showed a noticeable displacement. It is due to improvised geopolymer network organisation and there is more alkali cations present making the bonds to be less polar [18].

From the geopolymer spectra, the absorption band for v(Si-O-Si / Si-O-Al) strong bending vibration was observed at 523.94 cm^{-1} while a moderate IR band at 692.20 cm^{-1} was assigned as stretching vibrations of v (Si-O-Si/Si-O-Al) in geopolymer which is in close agreement with previous reported studies, as it is contributed to the stretching bands of tetrahedral aluminium [18]. Strong peaks from SBC around wavenumbers of 461.56 cm^{-1} and 531.33 cm^{-1} indicated montmorillonite structure which was then deconstructed and dissolved into Si-O and Al-O tetrahedral; characteristic of an amorphous aluminosilicate for geopolymer [20, 21].

Additionally, the presence of symmetrical v(Al-O) moderate vibration peak in AlO_4 with tetrahedral coordination can be observed at 789.88 cm^{-1} from the spectra of geopolymer [20]. Meanwhile, Li et al. highlighted that this modest peak can be attributed to Al-O-H bending vibrations or minor anionic ions such as silicate monomer, SiO^-. This is because the source material is rapidly dissolved forming small silicate monomers. The small peak seen in SBC spectra at 796.44 cm^{-1} disappeared in the geopolymer spectra, indicating that silicate monomers were consumed in favor of bulkier species [22].

The intense absorption band of asymmetrical Si-O/Al-O assigned at 1027.09 cm^{-1} is considered as the main absorption band. As the polycondensation process progresses, this band gets more concentrated, producing more aluminosilicates matrix. The band at 1027 cm^{-1} was likely due to an increase in the amount

of functional group attached to the molecular bond resulting in less non-bridging oxygen and Al being substituted in the silicate sites [18]. An absorption peak near 1600 cm^{-1} is attributed to bending vibration of (H-O-H) bonds, perhaps because the NaOH residue in the geopolymer which consequently produces Na_2CO_3 by interacting with CO_2 in the air [23].

Furthermore, the two absorption peaks in the 2800-3200 cm^{-1} range were the stretching vibrations of v(-Al-OH) and v(-Si-OH), indicating that tetrahedral structure was not damaged. This is mostly due to the evaporation of water in the paste that limited soluble ion movement, resulting in an inadequate reaction between clay precursor and the alkali activator [20]. It appeared that the band at approximately 3443.50 cm^{-1} is related to the stretching vibration of the O-H bond of geopolymer, whereas a comparable peak emerged at 3345.83 cm^{-1} for the SBC. The bands shifted likely because the usage of water during preparation of alkaline activator solution added with geopolymer slurry for geopolymerisation process. Considering water is a main byproduct of geopolymers, the results were comparable [24].

Carbon dioxide (CO_2) stretching vibration band at around 1300-1400 cm^{-1} was also discovered. These bands defined the geopolymer material [25]. These distinct peaks mostly indicate the presence of geopolymer compounds. The small-scale difference in intensity for the influence of carbonates was recorded at 1429.30 and 1387.02 cm^{-1}, corresponding to the stretching vibrations of O-C-O bonds in the carbonate group (CO_3^{2-}) caused by the carbonation reaction between carbon dioxide from the air and the geopolymer. The slight detected rise was caused by increased carbonation as a result of the high number of free ions. Carbonates contributed more to samples activated with sodium solution, which can react with atmospheric CO_2 to form Na_2CO_3 species [18].

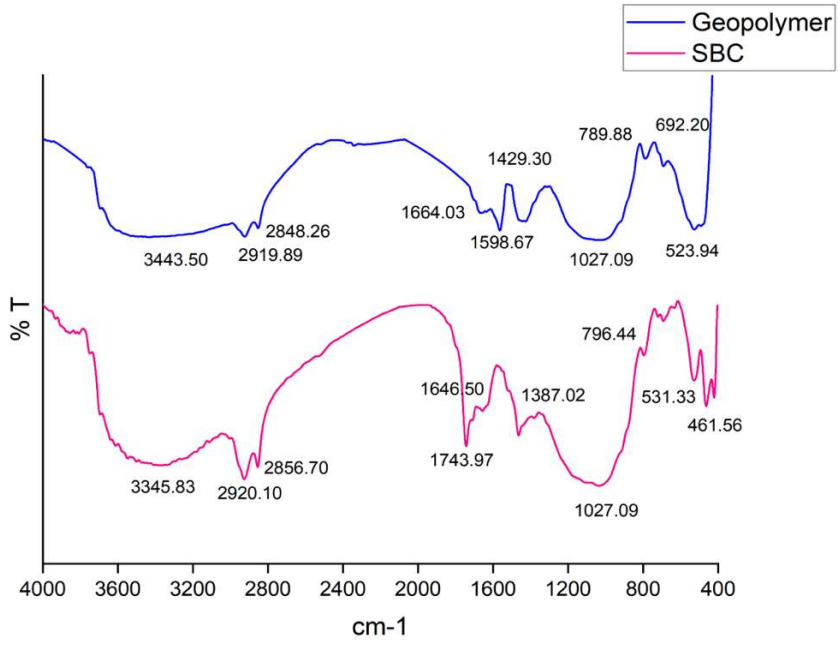

Figure 3. FTIR spectrum of geopolymer synthesized in this study and spent bleaching clay (SBC)

Surface morphology and elemental analysis

Figure 4 shows the SEM images of SBC and geopolymer. Figure 4 (a) shows that bulk, compact, and sponge-like structure are well formed for SBC. In contrast to other precursors, montmorillonite has a mainly fluffy and lumpy morphology, which may be characterised by the material's very amorphous structure caused by the dissolution of the multilayered plates structure [21,26]. This lumpy microstructure could be attributed to chemical modification in the clay galleries during palm oil refinement process. As a result, the composite is altered by an ionic liquid

(which is entrained oil and metallic contaminant) filled with aggregated montmorillonite particles that act as thickeners, and the ionic liquid completely form a thin film spread over the clay particles [27,28]. It also has a structure similar to illite, except that isomorphous substitution commonly occurs in the octahedral sheet, where every sixth aluminium is replaced by magnesium [21]. Figure 4 (b) shows an amorphous appearance with a rough, flaky, mild porous and less dense condition.

Additionally, the big lumps present in Figure 4 (b) exposes the homogenous part of sample. The aggregate seemed strongly bonded and a transition layer developed between SBC and the geopolymer matrix phase, indicating that a polymerisation process took place, generating a (-Al-O-Si-) chemical link. Thus, when a geopolymer substitutes the concrete, the alkali aggregated reaction does not induce product cracking [20]. Besides, the morphology of clay based geopolymer shifted to layer-like structure after geopolymerization process despite the curing temperature [19]. Meanwhile, the pores in geopolymers are mostly generated by water evaporation in the precursor. Pore structure parameters such as pore diameter, porosity, pore morphology and pore diameter uniformity have been shown to influence the microstructure and mechanical properties of geopolymers [29]. The rise of water absorption in geopolymer composition causing the microstructural deterioration, allowing water to exit the geopolymer network and be retained [30].

Spent bleaching clay (SBC) and geopolymer elemental composition were examined by using EDX analysis as per Table 2. The semi-quantitative elemental composition exposed the primary elements characterised were oxygen, carbon, silicon and aluminium with proportion values of 40.09%, 36.00%, 10.02% and 2.16% respectively, with traces of Ca, Fe, Mg, K and S. Based on these findings, the microstructure is primarily made up of amorphous sodium aluminosilicate binder (N- A-S-H) [31]. It is noteworthy that the composition of Na comprised almost 7% of the geopolymer's structure. Due to the alkali activator utilised during the geopolymerization reaction, the proportion of Na elements rose drastically [32,33]. Whilst, the Si molar ratios revealed the significance of binder phases in alkali activated geopolymers [31].

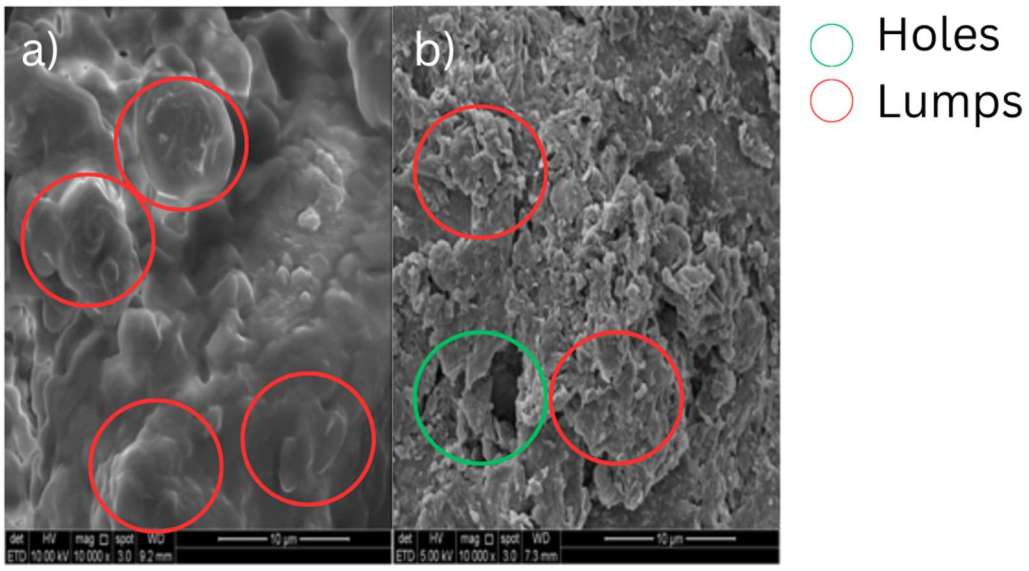

Figure 4. SEM image of (a) SBC and (b) geopolymer at 10,000x magnification

Table 2. EDX analysis of SBC and Geopolymer

Element	SBC (wt.%)	Geopolymer (wt.%)
O	22.95	40.09
C	64.40	36.00
Si	6.08	10.02
Na	NA	6.77
Al	1.57	2.16
Ca	0.81	1.85
Fe	3.57	1.74
Mg	0.62	0.64
K	NA	0.39
S	NA	0.34

Thermal analysis of neat and treated geopolymers

Figure 5 displays the thermogravimetric analysis and their differential curves for the neat and treated geopolymers developed in this work. From Figure 5, it was discovered that there is no discernible difference in the weight loss regardless of the curing method utilised. According to Gultekin and Ramyar, the geopolymers' free and weakly bonded-absorbed water caused the abrupt weight loss in the region of 0-200°C [34]. Another phenomenon, leading to the second weight loss, which occurs around 350°C, is the loss of hydroxyl from clay and organic residual oil, which makes up roughly 10-30% of the mass respective to the geopolymers. At 700 °C, this phase denotes the amorphization of the clay and the elimination of the montmorillonite precursor [1]. Dehydroxylation of the illite phase, the endothermic peak, begins at 600°C and concludes at 700°C, as can be shown in Figure 5 [35]. Besides, Marsh et al. stated that the continued curve is the formation of activated montmorillonite system [36].

Eventually, the presence of carbonates might also increase the compressive strength of geopolymer [37]. Besides, the unburnt organic carbon might be responsible for a mass loss of roughly < 1%, which were measured at the DTA peak of 170-180°C. Thermal analysis demonstrated that the clay-based geopolymers exhibited a thermally stable structure when heated up to 900°C. As a result of its improved thermal characteristics, SBC-based geopolymer may be more beneficial for manufacturing components that are stable at high temperatures than Portland cement systems. All in all, it can be summarised that all treated and untreated geopolymer samples possess good heat resistance, where it all decomposed only after 700°C.

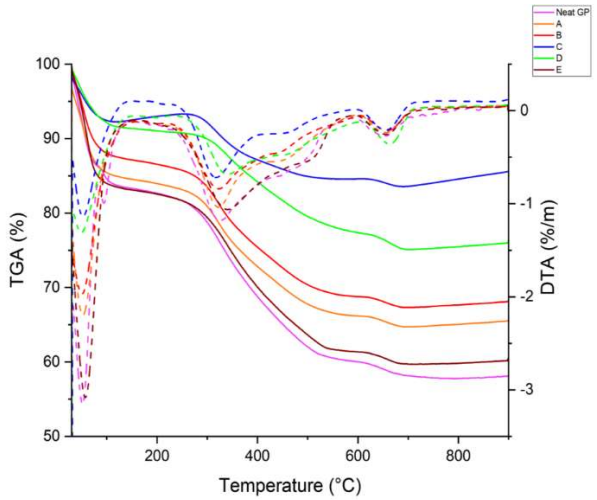

Figure 5. TGA-DTA of neat and treated geopolymer at different curing condition; water-cured (A-D) and ambient-cured (E)

Alkaline leachability via AAS

Geopolymer of same batch was tested for alkaline leachability from ambient curing and various liquid/solid (L/S) ratio as per Table 1 for water curing. Figure 6 depicts the concentration of sodium in the leachate after 28 days of leaching.

It is noticed that with increasing L/S ratio, there was a further drop in Na^+ leaching. This is because the increased of soluble silicate content in the geopolymer matrix probably results in less alkali leaching, which is consistent with water absorption values [38]. The less compact microstructure leads to fewer sodium associated in charge balancing sites. As a result of the porosity effects, the leaching of Na^+ is substantially enhanced [39]. This shows that resistance to efflorescence requires both decreased porosity and sodium incorporation in charge balancing sites [38].

As per Figure 6, alkaline leaching ability of geopolymer samples treated with L/S ratio of 2:1 is greater than for other samples with higher L/S ratios. Despite having a variable L/S ratio, samples C and D released nearly less Na^+ and at a slower rate in the leaching tests. Meanwhile, for all water-cured specimens, the leaching process significantly reduced the total alkali leaching after 28 days of immersion as compared to ambient-cured specimen. This is possibly due to the NaOH concentration in the sample and solution leveled off more slowly when pouring higher quantities of sample, in other words, more effective diffusion [3].

Besides, leaching behavior reduced for water-cured samples according to the L/S ratio from 2:1 to 20:1. Due to the high solution concentration of water content, the diffusion and mass transfer velocity were quick during the initial stage of leaching. The specimen surfaces begin to be progressively covered in residue as the reaction goes on and the concentration of the solution also starts to decrease. On account to this, the diffusion and mass transfer velocity slowed down, which given the lesser concentration that was leached out, indicated that the leachate solubility was also decreased [40]. Overall, water-cured specimen, sample A, with L/S ratio of 2:1 exhibited the most sodium ions leached from geopolymer as compared to other specimens.

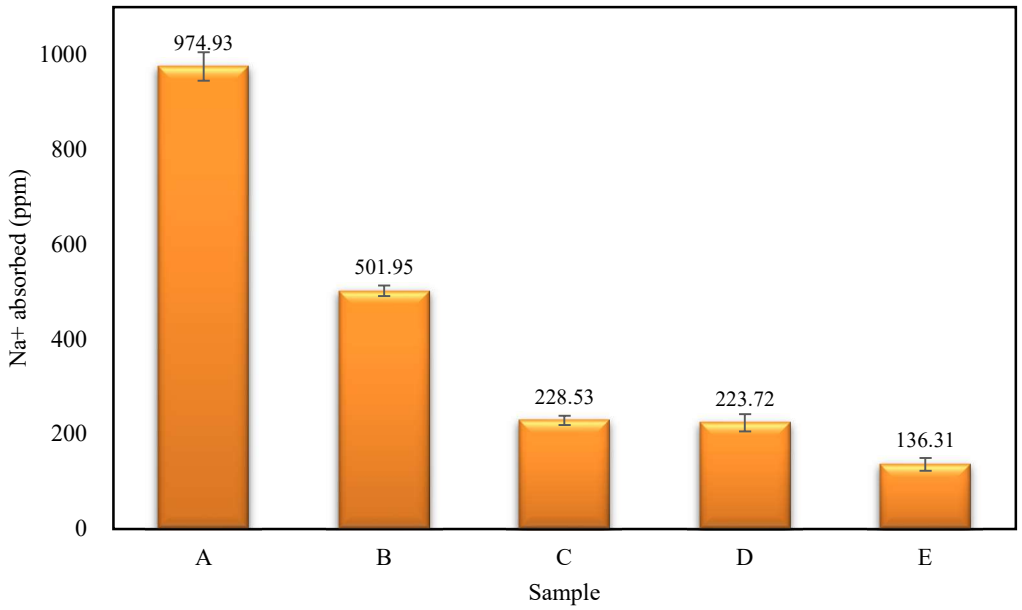

Figure 6. Sample A-D are water-cured specimens while E is ambient-cured specimen. Liquid/solid (L/S) ratio for water-cured specimens of A is 2:1, B is 4:1, C is 10:1 and D is 20:1

Alkaline leachability via EIS

The AC impedance spectra, also known as Nyquist plot, of treated geopolymers after 28 days of curing shown in Figure 7. It illustrates the oblique lines, which increases gradually due to ion diffusion effect. The resultant Nyquist plot shifts from left to right as curing age grows, and the value of resistance, which refers to the actual impedance of the junction, also rises. The elevation in resistance reflects the mobility of ions in the individual specimens, which in accordance with the L/S ratio [41]. On account to this, Biondi et al. reported that when immersed in water, Na^+ ions, as well as silicon and chloride ions, migrate in small amounts from the geopolymer [42]. According to Song et al., the parameter, θ linked to the surface condition of the montmorillonite particles and the applied voltage, E are the two key factors affecting the current of the geopolymer slurry. The θ represents the relationship between the dissolved surface area and the combined surface area of the montmorillonite particles. Consequently, an increase in θ will cause a rise in plasma current [43]. Therefore, the Nyquist plot from sample D with L/S ratio of 20:1 reflected highest impedance real part data to those of other ratios. This is because during the soaking phase, oxygen vacancies that have diffused from the solution interface to the geopolymer interface essentially promotes the formation of the leachates with high ion concentrations [44].

Charges in pore solution could be conveyed over the surface of the solid phase due to the differing resistance characteristics of solid and liquid phases [41]. Also, the concentration of ions in the geopolymer slurry rises as Si and Al dissolve, progressively increasing the resistance value of the sample. Furthermore, ambient-cured specimen, sample E, yield increased impedance response due to excellent electrolyte interfacial contact, probably anticipated to OH^- concentration solubility [45]. Potentially, the sample should have developed more aluminosilicate bonds during the curing phase. Therefore, sample A is considered to indicate excellent resistance in alkaline leaching since the other samples likely to have charge transferred in its solution.

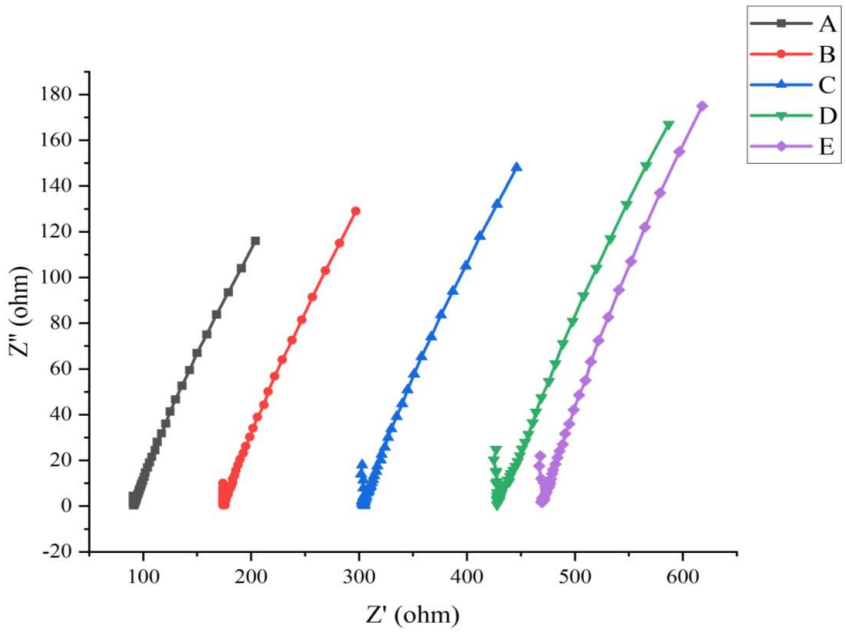

Figure 7. EIS responses in Nyquist curve at various curing condition; water-cured (A-D) and ambient-cured (E)

Conclusion

Aluminosilicates polymerised in an alkaline media at elevated temperature, produce a substance with cementitious characteristics. Spent bleaching clay-based geopolymer has been successfully designed by geopolymerisation, characterised and evaluated towards investigating the efflorescence development by using the leachability methods. This study details an

effort to investigate the alkaline leachability which causes the efflorescence phenomena on geopolymers using AAS and EIS. Mineralogically, the efflorescence still has impact on the main amorphous gels and residual crystalline phases formed from montmorillonite, which make up the majority of the clay-based geopolymers. According to this finding, free alkali concentration is significantly influenced by the alkalinity of the activating solution. Despite favouring the mechanical strength of the goods, higher alkalinities tend to enhance the leachability. Hence, sample A (L/S ratio 2:1) was analysed to have the most prominent curing condition to work towards efflorescence formation. In addition, the compound was analysed via several spectroscopic and analytical techniques, namely infrared (FT-IR), scanning electron microscopy (SEM-EDX), and thermogravimetric-differential thermal analysis (TGA-DTA). The montmorillonite based geopolymer in this study have significant thermal stability, as for both water and ambient-cured specimens yielded less weight loss as compared to neat geopolymer indeed. It is compatible with the outcome that high water and NaOH concentration reduces the strength of geopolymers to yield low compressive strength and a mild porous structure. On the other hand, studies on efflorescence propensity via AAS and EIS have demonstrated that curing geopolymers in water conditions is an efficient way to reduce efflorescence formed on their surface. This is due to the most Na^+ being leached away in sample A, liquid/solid (L/S) 2:1 ratio, with also an adequate thermal stability and impedance response. It is also demonstrated that ambient curing could not act preferably as a suggested curing condition with utmost exhibition.

Acknowledgement

This work was supported by the Research University (RUI) Grant (1001/PKIMIA/8011137) from Universiti Sains Malaysia.

References

1. Majdoubi, H., Haddaji, Y., Mansouri, S., Alaoui, D., Tamraoui, Y., Semlal, N., Oumam, M., Manoun, B. and Hannache, H. (2021). Thermal, mechanical and microstructural properties of acidic geopolymer based on moroccan kaolinitic clay. *Journal Building Engineering*, 35:102078.
2. Janošević, N., Đorić-Veljković, S., Topličić-Ćurčić, G. and Karamarković, J. (2018). Properties of geopolymers. *Facta Universitatis, Series: Architecture and Civil Engineering,* 16(1): 045-056.
3. Łach, M., Korniejenko, K., Walter, J., Stefańska, A. and Mikuła, J. (2020). Decreasing of leaching and improvement of geopolymer properties by addition of aluminum calcium cements and titanium oxide. *Materials,* 13(3): 495.
4. Abdul Rahim, R. H., Rahmiati, T., Azizli, K. A., Man, Z., Nuruddin, M. F. and Ismail, L. (2015). Comparison of using NaOH and KOH activated fly ash-based geopolymer on the mechanical properties. In Materials science forum (Vol. 803, pp. 179-184). Trans Tech Publications Ltd.
5. Memon, F. A., Nuruddin, M. F., Khan, S., Shafiq, N. A. S. I. R. and Ayub, T. (2013). Effect of sodium hydroxide concentration on fresh properties and compressive strength of self-compacting geopolymer concrete. *Journal Engineering Science Technology,* 8(1): 44-56.
6. Tuyan, M., Andiç-Çakir, Ö. and Ramyar, K. (2018). Effect of alkali activator concentration and curing condition on strength and microstructure of waste clay brick powder-based geopolymer. *Composites Part B: Engineering,* 135: 242-252.
7. Hatami, A. M., Sabour, M. R. and Amiri, A. (2018). Recycling process of spent bleaching clay: Optimization by response surface methodology. *Global Journal of Environmental Science and Management,* 4(1): 9-18.
8. Sedghamiz, M. A., Attar, F. and Raeissi, S. (2019). Experimental investigation of acid regeneration of spent bleaching clay de-oiled by the in-situ transesterification process at various operating conditions. *Process Safety and Environmental Protection,* 124: 121-127.
9. Loh, S. K., Cheong, K. Y. and Salimon, J. (2017). Surface-active physicochemical characteristics of spent bleaching earth on soil-plant interaction and water-nutrient uptake: A review. *Applied Clay Science,* 140: 59-65.
10. Zhang, C., Yu, M., Li, X., Li, X., Siyal, A. A., Liu, Y., ... and Li, Y. (2022). Disposal, regeneration and

pyrolysis products characterization of spent bleaching clay from vegetable oil refinery in a fluidized bed pyrolyser. *Journal of Cleaner Production,* 346: 131157.

11. Saludung, A., Azeyanagi, T., Ogawa, Y. and Kawai, K. (2021). Alkali leaching and mechanical performance of epoxy resin-reinforced geopolymer composite. *Materials Letters,* 304: 130663.
12. Škvára, F., Kopecký, L., Šmilauer, V. and Bittnar, Z. (2009). Material and structural characterization of alkali activated low-calcium brown coal fly ash. *Journal of Hazardous Materials*, 168(2-3): 711-720.
13. Ying, M. W., Azmi, M. and Ganesan, S. (2022). Synthesis and characterization of spent bleaching clay-based geopolymer: an effort towards palm oil industry waste reutilization. *Chemistry–An Asian Journal,* 17(14): e202200286.
14. Shehata, N., Sayed, E. T. and Abdelkareem, M. A. (2021). Recent progress in environmentally friendly geopolymers: A review. *Science of the Total Environment,* 762: 143166.
15. Zhang, Z., Provis, J. L., Reid, A. and Wang, H. (2014). Fly ash-based geopolymers: The relationship between composition, pore structure and efflorescence. *Cement and Concrete Research*, 64: 30-41.
16. Liew, Y. M., Heah, C. Y. and Kamarudin, H. (2016). Structure and properties of clay-based geopolymer cements: A review. *Progress in Materials Science,* 83: 595-629.
17. Tchadjie, L. N. and Ekolu, S. O. (2018). Enhancing the reactivity of aluminosilicate materials toward geopolymer synthesis. *Journal of Materials Science*, 53(7): 4709-4733.
18. Finocchiaro, C., Barone, G., Mazzoleni, P., Leonelli, C., Gharzouni, A. and Rossignol, S. (2020). FT-IR study of early stages of alkali activated materials based on pyroclastic deposits (Mt. Etna, Sicily, Italy) using two different alkaline solutions. *Construction and Building Materials,* 262: 120095.
19. Abdullah, M. M. A. B., Ming, L. Y., Yong, H. C. and Tahir, M. F. M. (2018). Clay-based materials in geopolymer technology. *Cement Based Materials,* 239: 77438.
20. Shi, H., Ma, H., Tian, L., Yang, J. and Yuan, J. (2020). Effect of microwave curing on metakaolin-quartz-based geopolymer bricks. *Construction and Building Materials,* 258: 120354.
21. Okashah, A. M., Zainal, F. F., Hayazi, N. F., Nordin, M. N. and Abdullah, A. (2021). Pozzolanic properties of calcined clay in geopolymer concrete: A review. In AIP Conference Proceedings (Vol. 2339, No. 1). AIP Publishing.
22. Li, Z., Zhang, S., Zuo, Y., Chen, W. and Ye, G. (2019). Chemical deformation of metakaolin based geopolymer. *Cement and Concrete Research,* 120: 108-118.
23. Feng, B., Liu, J., Chen, Y., Tan, X., Zhang, M. and Sun, Z. (2022). Properties and microstructure of self-waterproof metakaolin geopolymer with silane coupling agents. *Construction and Building Materials,* 342: 128045.
24. Zawrah, M. F., Sawan, S. A., Khattab, R. M. and Abdel-Shafi, A. A. (2020). Effect of nano sand on the properties of metakaolin-based geopolymer: Study on its low rate sintering. *Construction and Building Materials,* 246: 118486.
25. Zidi, Z., Ltifi, M. and Zafar, I. (2021). Synthesis and attributes of nano-SiO_2 local metakaolin based-geopolymer. *Journal of Building Engineering,* 33: 101586.
26. Salahudeen, N. (2018). Metakaolinization effect on the thermal and physiochemical propperties of kankara kaolin. *Applied Science and Engineering Progress,* 11(2): 127-135.
27. Cecilia, J. A., García-Sancho, C. and Franco, F. (2013). Montmorillonite based porous clay heterostructures: Influence of Zr in the structure and acidic properties. *Microporous and Mesoporous Materials,* 176: 95-102.
28. Alekseeva, O., Noskov, A., Grishina, E., Ramenskaya, L., Kudryakova, N., Ivanov, V. and Agafonov, A. (2019). Structural and thermal properties of montmorillonite/ionic liquid composites. *Materials,* 12(16): 2578.
29. Chen, X., Zhu, G., Zhou, M., Wang, J. and Chen, Q. (2018). Effect of organic polymers on the properties of slag-based geopolymers. *Construction and Building Materials,* 167: 216-224.

30. Boum, R. B. E., Kaze, C. R., Nemaleu, J. G. D., Djaoyang, V. B., Rachel, N. Y., Ninla, P. L., ... and Kamseu, E. (2020). Thermal behaviour of metakaolin–bauxite blends geopolymer: microstructure and mechanical properties. *SN Applied Sciences,* 2(8):1358.
31. Nemaleu, J. G. D., Bakaine Djaoyang, V., Bilkissou, A., Kaze, C. R., Boum, R. B. E., Djobo, J. N. Y., ... and Kamseu, E. (2022). Investigation of groundnut shell powder on development of lightweight metakaolin based geopolymer composite: mechanical and microstructural properties. *Silicon,* 14(2): 449-461.
32. Aouan, B., Alehyen, S., Fadil, M., Alouani, M. E., Khabbazi, A., Atbir, A. and Taibi, M. H. (2021). Compressive strength optimization of metakaolin-based geopolymer by central composite design. *Chemical Data Collections,* 31:100636.
33. El Alouani, M., Alehyen, S. and El Achouri, M. (2019). Preparation, characterization, and application of metakaolin-based geopolymer for removal of methylene blue from aqueous solution. *Journal of Chemistry,* 2019: 4212901.
34. Gultekin, A. and Ramyar, K. (2022). Effect of curing type on microstructure and compressive strength of geopolymer mortars. *Ceramics International,* 48(11): 16156-16172.
35. Nmiri, A., Hamdi, N., Yazoghli-Marzouk, O., Duc, M. and Srasra, E. (2017). Synthesis and characterization of kaolinite-based geopolymer: Alkaline activation effect on calcined kaolinitic clay at different temperatures. *Journal Materials Environmental Sciences,* 8(2): 276-290.
36. Marsh, A., Heath, A., Patureau, P., Evernden, M. and Walker, P. (2018). Alkali activation behaviour of un-calcined montmorillonite and illite clay minerals. *Applied Clay Science,* 166: 250-261.
37. Jaradat, Y. and Matalkah, F. (2021). Olive biomass ash-based geopolymer composite: development and characterisation. *Advances in Applied Ceramics,* 120(1): 1-9.
38. Longhi, M. A., Zhang, Z., Walkley, B., Rodríguez, E. D. and Kirchheim, A. P. (2021). Strategies for control and mitigation of efflorescence in metakaolin-based geopolymers. *Cement and Concrete Research,* 144: 106431.
39. Zhang, Z., Provis, J. L., Ma, X., Reid, A. and Wang, H. (2018). Efflorescence and subflorescence induced microstructural and mechanical evolution in fly ash-based geopolymers. *Cement and Concrete Composites,* 92: 165-177.
40. Tigue, A. A. S., Malenab, R. A. J., Dungca, J. R., Yu, D. E. C. and Promentilla, M. A. B. (2018). Chemical stability and leaching behavior of one-part geopolymer from soil and coal fly ash mixtures. *Minerals,* 8(9): 411.
41. Hu, X., Shi, C., Liu, X. and Zhang, Z. (2020). Studying the effect of alkali dosage on microstructure development of alkali-activated slag pastes by electrical impedance spectroscopy (EIS). *Construction and Building Materials,* 261: 119982.
42. Biondi, L., Perry, M., McAlorum, J., Vlachakis, C. and Hamilton, A. (2020). Geopolymer-based moisture sensors for reinforced concrete health monitoring. *Sensors and Actuators B: Chemical,* 309: 127775.
43. Song, Q., Wang, J., Dong, T., Hel, L. and Lu, S. (2019). Study of the Alkali activated Geopolymer by AC Impedance Spectroscopy. *In IOP Conference Series: Earth and Environmental Science* (Vol. 267, No. 2, p. 022001). IOP Publishing.
44. Fan, L. F., Zhong, W. L. and Zhang, Y. H. (2022). Effect of the composition and concentration of geopolymer pore solution on the passivation characteristics of reinforcement. *Construction and Building Materials,* 319: 126128.
45. Pengou, M., Ngouné, B., Tchakouté, H. K., Nanseu, C. P. and Ngameni, E. (2020). Utilization of geopolymer cements as supercapacitors: influence of the hardeners on their properties. *SN Applied Sciences,* 2: 1-7.